RSC Advances

Hydrolytically active tetranuclear [Ni^{II}$_2$]$_2$ complexes: synthesis, structure, spectroscopy and phosphoester hydrolysis

Gopal C. Giri,^{a} Ayan Patra,^{a} Gonela Vijaykumar,^{b} Luca Carrella,^{c} and Manindranath Bera^{*a}

^{a}*Department of Chemistry, University of Kalyani, Kalyani, West Bengal-741235, INDIA. E-mail: mbera2009@klyuniv.ac.in; http://www.klyuniv.ac.in; Fax: +91 33 25828282; Tel: +91 33 25828282 x306*
^{b}*Department of Chemical Sciences, Indian Institute of Science Education & Research Kolkata, Mohanpur, West Bengal-741246, INDIA.*
^{c}*Institut fur Anorganische Chemie und Analytische Chemie, Johannes-Gutenberg Universität Mainz, Duesbergweg 10-14, D-55128 Mainz, Germany.*

Abstract

Three tetranuclear nickel(II) complexes, [Ni$_4$(H$_2$chdp)$_2$(H$_2$O)$_4$]Br$_2$·4CH$_3$OH·3H$_2$O (**1**), [Ni$_4$(H$_2$chdp)$_2$(H$_2$O)$_4$](PF$_6$)$_2$ (**2**) and [Ni$_4$(H$_2$chdp)$_2$(H$_2$O)$_4$](ClO$_4$)$_2$·3.2CH$_3$OH·0.8H$_2$O (**3**) have been synthesized by exploiting the flexibility, chelating ability and bridging potential of a new symmetrical μ-bis(tetradentate) ligand, H$_5$chdp (H$_5$chdp = *N,N'*-Bis[2-carboxybenzomethyl]-*N,N'*-Bis[2-hydroxyethyl]-1,3-diaminopropan-2-ol). Complexes **1**, **2** and **3** have been synthesized by carrying out reaction of the ligand H$_5$chdp with stoichiometric amounts of NiCl$_2$·6H$_2$O/NaBr, NiCl$_2$·6H$_2$O/NH$_4$PF$_6$, and Ni(ClO$_4$)$_2$·6H$_2$O, respectively, in methanol-water in the presence of NaOH at ambient temperature. Characterizations of the complexes have been done using various analytical techniques including single crystal X-ray structure determination of complexes **1** and **3**. Molecular architecture of each complex is built from the self-assembly of two monocationic [Ni$_2$(H$_2$chdp)(H$_2$O)$_2$]$^+$ units which are exclusively bridged by two benzoate functionalities of the ligands. Single crystal X-ray structure analyses reveal that the metallic cores of complexes **1** and **3** consist of four distorted octahedral nickel(II) ions with intra-ligand Ni---Ni separation of 3.527(7) Å and 3.507(1) Å, respectively. Complexes **1** and **3** display a rare μ_3:η^2:η^1:η^1 bridging mode of two benzoate groups of H$_2$chdp^{3-} ligand with each bridging among three nickel(II) ions. Mass spectrometric analyses suggest that all the tetranuclear complexes are stable in solution. Potentiometric titration results and the corresponding species distribution curves show that all the

1

complexes exist predominantly in their tetrameric species in solution, in the pH range of 6-12. The catalytic activity of all the three complexes toward phosphoester hydrolysis has been investigated in methanol-water (1:1; v/v) solution by UV-Vis spectrophotometric technique using bis(*p*-nitrophenyl) phosphate (BNPP) as a model substrate.

Introduction

The group of multimetallic complexes is a consolidated family within the area of supramolecular coordination chemistry.[1,2] The stereochemical preferences of metal ions in combination with diverse binding possibilities of the ligands have produced a large variety of such complexes. The neighboring metal centers in multimetallic systems are expected to cooperate in promoting reactions, and new electronic interactions might lead to distinct physical properties. Cooperative interactions have commonly been observed in biological systems, and nature has constructed numerous multimetallic protein complexes that perform an extraordinary array of catalytic transformations.[3-6] In this context, there is a growing interest in the active site structures and catalytic functions of nickel(II) containing metalloenzymes.[7] Among these, urease is an enzyme that catalyzes the hydrolysis of urea to ammonia and carbamic acid by utilizing carbamylated lysine bridged dimetallic centers of nickel(II) ions in the active site.[8-11] This enzymatic conversion of urea to ammonia and carbamic acid has shown a considerable importance in the field of agricultural and medicinal chemistry.[11,12] Moreover, multinuclear nickel(II) complexes are relatively well-known for exhibiting magnetic interactions that are antiferro- or ferromagnetic in nature.[13-23] In these complexes, controlling the interactions among the metal ions provides a way to organize the overall spin ground state. Consequently, this can have a significant implication on their magnetic behavior.[24,25]

The focus here is on a new symmetrical μ-bis(tetradentate) ligand, H$_5$chdp incorporating two benzoate and two hydroxyethyl functionalities. Similar carboxylate-rich polydentate ligands have been used as a way to assemble different metal ions into aggregates with relevance in the area of bioinorganic chemistry.[26-30] For example, a carboxylate-rich polydentate ligand containing two benzoate and two acetate groups is known to bind cobalt(II), copper(II) and zinc(II) ions to produce mono-, di-, tetra- and hexanuclear complexes showing the bridging potential of carboxylates.[26,27,31-33] Recently,

the unusual amide binding modes of a similar amide and carboxylate-rich polydentate ligand has been explored in a self-assembled heptanuclear zinc(II) complex.[34] Very recently, we have also reported the synthesis, characterization and *in vitro* biological investigations on human cervical cancer cells (HeLa) of new water soluble heteronuclear [NaCu$^{II}_6$] metallomacrocyclic sandwich complexes using a similar carboxylate and pyridine containing polydentate ligand.[29] In this paper, we report the synthesis, X-ray crystal structure, spectroscopic characterization and phosphoester hydrolysis of three new tetranuclear nickel(II) complexes.

Results and discussion

Synthesis and general characterization

The new symmetrical μ-bis(tetradentate) ligand, H$_5$chdp has been synthesized in two step reactions (Scheme 1). The synthesis of the precursor ligand, H$_3$cdp has been achieved by the condensation of stoichiometric amounts of 2-carboxybenzaldehyde and 1,3-diamino-propan-2-ol in the presence of NaOH in methanol under refluxing conditions for 4 h, followed by the subsequent reduction using NaBH$_4$. Acidification of the resulting solution by addition of conc. HCl to pH~5 produced a white solid product. The product has been characterized to be a reduced Schiff base ligand, H$_3$cdp·H$_2$O by elemental analysis, FTIR and NMR spectroscopy. Alkylation of the secondary amines of H$_3$cdp with 2-iodoethanol in 1:2.5 molar ratio yielded the symmetrical μ-bis(tetradentate) ligand, H$_5$chdp, in good yield. The ligand, H$_5$chdp has been fully characterized using the analytical techniques such as elemental analysis, FTIR (Fig. S1, Supporting Information), ^{1}H and ^{13}C NMR (Figs. S2 and S3, Supporting Information), and ESI mass spectrometric (Fig. S4, Supporting Information) techniques. Very recently, we have shown that the alkylation of the secondary amine at one half of H$_3$cdp with 2-iodoethanol in 1:1 molar ratio and intramolecular cyclization between the secondary amine and the benzoate functionality at the other half produces the unsymmetrical dinucleating ligand consisting of an isoindol functionality.[35] The ligand, H$_5$chdp has been chosen for the present investigation because the central pendant alcoholic arm of this ligand acts as a spacer-cum-bridging unit between the two metal ions in the dinuclear entity. Therefore, we

3

decided to prepare such a ligand that may adequately mimic the ligand environment of di- and tetranuclear nickel(II) active sites in metallohydrolases.

The reaction of H_5chdp with $NiCl_2 \cdot 6H_2O$ and NaBr in 1:2:1 molar ratio in the presence of a strong base, NaOH in methanol-water at room temperature afforded a light green tetranuclear complex, $[Ni_4(H_2chdp)_2(H_2O)_4]Br_2 \cdot 4CH_3OH \cdot 3H_2O$ (**1**) (Scheme 2). The reaction of H_5chdp with $NiCl_2 \cdot 6H_2O$ and NH_4PF_6 in 1:2:1 molar ratio in the presence of NaOH in methanol-water at room temperature yielded a green tetranuclear complex, $[Ni_4(H_2chdp)_2(H_2O)_4](PF_6)_2$ (**2**) (Scheme 2). Similarly, the reaction of H_5chdp with $Ni(ClO_4)_2 \cdot 6H_2O$ in 1:2 molar ratio in the presence of NaOH, in methanol-water at room temperature produced a green complex, $[Ni_4(H_2chdp)_2(H_2O)_4](ClO_4)_2 \cdot 3.2CH_3OH \cdot 0.8H_2O$ (**3**) (Scheme 2). They represent a new family of μ-alkoxo-μ_3-carboxylato bridged tetranuclear nickel(II) clusters. Characterizations of the complexes were done by elemental analysis, FTIR, UV-Vis, mass spectrometric and potentiometric titration techniques. Furthermore, the molecular structures of complexes **1** and **3** were confirmed by single crystal X-ray analyses.

Crystal and molecular structures of complexes 1 and 3

Complex **1** crystallizes in a triclinic system and the structure was solved in *P*-1 space group. Complex **3** crystallizes in an orthorhombic system and the structure was solved in *Pbca* space group. The crystal structure of complex **1** consists of a cationic $[Ni_4(H_2chdp)_2(H_2O)_4]^{2+}$ species along with two Br$^-$ ions as the counter anions. Four methanol and three water molecules cocrystallized with the complex. The crystal structure of complex **3** consists of a cationic $[Ni_4(H_2chdp)_2(H_2O)_4]^{2+}$ species along with two ClO$_4^-$ ions as the counter anions. Three and one-fifth methanol, and four-fifth water molecules cocrystallized with the complex. The structural views of the cations of complexes **1** and **3** are depicted in Figs. 1 and 2. Each cationic species contains four Ni(II) ions, two H_2chdp^{3-} ligands and four H_2O molecules. The tetranuclear complex cation is formed through the self-assembly of two dimeric $[Ni_2(H_2chdp)]^+$ units exclusively bridged by two $\mu_3:\eta^2:\eta^1:\eta^1$ benzoate groups of the two H_2chdp^{3-} ligands. Each dimer consists of two Ni(II) ions which are bridged by the central alkoxo oxygen atom of H_2chdp^{3-} ligand and one benzoate group of the other H_2chdp^{3-} ligand of opposite Ni_2

4

moiety. Each dimer also takes the similar structural arrangements with respect to the coordination mode of H_2chdp^{3-} ligand. Two terminal aliphatic alcoholic arms of H_2chdp^{3-} ligand within each Ni_2 dimer of complexes **1** and **3** are oriented in a *trans* fashion (Figs. 3 and 4).

Interestingly, complexes **1** and **3** display a rare $\mu_3:\eta^2:\eta^1:\eta^1$ tridentate bridging mode of two carboxylate groups with each bridging among three Ni(II) ions. The *syn-syn* and *syn-anti* bidentate bridges are commonly observed in dinuclear or polynuclear metal carboxylate chemistry.[36] However, the tridentate bridges in metal-carboxylate complexes are not common.[37] There are three coordination modes in tridentate bridging (Scheme 3). The mode A is postulated to be an important intermediate in "carboxylate shift" chemistry,[37] mode B (a monodentate and a *syn-syn* bidentate bridges) has been found in metal-carboxylate complexes,[38] and mode C (a monodentate and a *syn-anti* bidentate bridges) has also been found in metal-carboxylate chemistry.[39] The current study offers a rare example with mode B carboxylate binding, in which the carboxylate group shows a tridentate bridging mode with a monodentate and a *syn-syn* bidentate bridges among the Ni(II) ions.

The coordination environment around the nickel(II) centers within each dimer exhibits distorted octahedral geometry. In complex **1**, the square base of the octahedral geometry around the Ni1 center is defined by the O1, O5, O5^i and N2 atoms, whereas that around the Ni2 center is defined by the O1, O4, O9 and N4 atoms. Whereas the axial positions of the octahedral geometry around the Ni1 center are occupied by the O11 and O12 atoms, the axial positions around Ni2 center are taken by the O2 and O10 atoms. Similarly, in complex **3**, the square base of the octahedral geometry around the Ni1 center is defined by the O20, O34, O34^i and N15 atoms, whereas that around the Ni2 center is formed by the O20, O35^i, O37 and N11 atoms. The axial positions of the octahedral geometry around the Ni1 center are occupied by the O18 and O36 atoms, and the axial positions around the Ni2 center are occupied by the O23 and O26 atoms. The average Ni-$O_{terminal\ alcohol}$, Ni-O_{aquo} and Ni-$O_{terminal\ carboxylate}$ bond distances are 2.124, 2.104 and 2.039 Å, respectively, which are comparable to the bond distances observed in similar octahedral nickel(II) complexes.[7,17,40,41] In complexes **1** and **3**, the intra-ligand Ni---Ni distances are 3.527(7) and 3.507(1) Å,[7,17,40,41] and the inter-ligand Ni---Ni distances are

3.106(8) and 3.117(1) Å, respectively. The comparable nickel-alkoxo and nickel-carboxylate arms provide the framework to support the wide Ni-O$_{alkoxo}$-Ni bridging angles of 129.1(1) and 127.3(1)° in complexes **1** and **3**, respectively, which are open enough to afford further coordination of carboxylates of the H$_2$chdp^{3-} ligand among the Ni(II) ions in a μ_3:η^2:η^1:η^1 fashion.

Spectroscopic studies

The different coordination modes of benzoates, namely, monodentate terminal and tridentate μ_3:η^2:η^1:η^1 bridging coordination in the complexes have been established by their FTIR spectra (Fig. S5, Supporting Information). Deacon and Phillips have carefully scrutinized the FTIR spectra of many carboxylate containing metal complexes with known X-ray crystal structures and drawn useful conclusion for the correlation between carboxylate stretching frequencies and their geometries.[42] In the FTIR spectra, three strong asymmetric v_{as}(COO$^-$) vibrations were observed at 1631, 1586 and 1559 cm^{-1}; 1629, 1593 and 1548 cm^{-1}; 1630, 1589 and 1555 cm^{-1}; whereas three strong symmetric v_s(COO$^-$) vibrations were observed at 1454, 1386 and 1365 cm^{-1}; 1465, 1404 and 1340 cm^{-1}; 1451, 1401 and 1368 cm^{-1} for complexes **1**, **2** and **3**, respectively. The significantly higher differences of Δ (Δ = v_{as}(COO$^-$) - v_s(COO$^-$)) of ~245 and 194, 225 and 208, and 229 and 187 cm^{-1} between the asymmetric and symmetric stretching vibrations are attributed to the monodentate terminal and monodentate bridging coordinations of benzoate groups in complexes **1**, **2** and **3**, respectively.[43] The relatively lower values of Δ at ~132, 128 and 138 cm^{-1} between the asymmetric and symmetric stretching vibrations are characterized by the *syn-syn* bidentate bridging (μ_2:η^1:η^1) of benzoate groups in complexes **1**, **2** and **3**, respectively.[43] In the FTIR spectrum of complex **2**, a prominent broad band centered at ~ 845 cm^{-1} and a strong sharp band at ~ 565 cm^{-1} can be assigned to the stretching and bending modes of the PF$_6^-$ ion, respectively.[44] A characteristic strong band (v_{ClO4}^-) has been observed at ~1089 cm^{-1} in the spectrum of complex **3**, suggesting the presence of perchlorate ion outside the coordination sphere.[45] In addition, the FTIR spectra of all the complexes exhibit a broad absorption band at ~ 3413 cm^{-1} which is assignable to the v(O-H) vibration of the coordinated alcohol groups and/or water molecules.

The electronic spectra of complexes **1**, **2** and **3** in methanol-water (1:1; v/v) at pH~7.5 display a broad absorption band in the visible region at 683 nm (ε, 138 $M^{-1}cm^{-1}$), 685 nm (ε, 146 $M^{-1}cm^{-1}$) and 658 nm (ε, 154 $M^{-1}cm^{-1}$), respectively, due to the weak d-d transitions (Fig. S6(a), Supporting Information). This is typical for d-d transitions of Ni(II) ions with an octahedral coordination environment. In addition, the spectra also show the distinct nickel(II) ion bound ligand-based charge transfer transitions at 276 nm (ε, 1391 $M^{-1}cm^{-1}$) and 220 nm (ε, 6971 $M^{-1}cm^{-1}$), 277 nm (ε, 1430 $M^{-1}cm^{-1}$) and 223 nm (ε, 7530 $M^{-1}cm^{-1}$), and 279 nm (ε, 1285 $M^{-1}cm^{-1}$) and 225 nm (ε, 6529 $M^{-1}cm^{-1}$), respectively (Fig. S6(b), Supporting Information). Thus, spectral comparison of three complexes indicates that they are structurally alike.

To be better acquainted with the structural features of the complexes in solution, the ESI mass spectra of all the complexes were recorded in methanol-water at pH~7.5. The solutions of complexes **1**, **2** and **3** were positive-ion electrosprayed into a quadrupole ion-trap mass spectrometer and subjected to collision-induced dissociation. The mass spectra of all the complexes exhibit the signal at m/z = 1119 corresponding to the tetranuclear $\{[Ni_4(H_2chdp)(Hchdp)]\}^+$ species. The spectra also display an intense signal at m/z = 560 (1119/2 = 559.5) matching to the tetranuclear $\{[Ni_4(H_2chdp)(Hchdp)]\}^{2+}$ species. The representative mass spectra of complexes **1**, **2** and **3** are shown in Figs. S7, S8 and S9 of the Supporting Information. The experimental and simulated spectra of the main peaks of complexes **1** and **3** are provided in Figs. S10 and S11 of the Supporting Information. The distribution patterns between the experimental and the simulated data are in good agreement to one another. To make sure whether any dimeric species is present in solution or not, MS/MS study of the peak at m/z = 1119 has been preformed for complex **1**. The MS/MS spectrum of complex **1** is shown in Fig. S12 of the Supporting Information. The MS/MS spectrum indicates that there is no any dimeric form of complex **1** present in solution. The signals at m/z = 1075, 1031, 987 and 943 in the MS/MS spectrum correspond to the species obtained upon successive decarboxylation (loss of four CO_2 molecules) of $\{[Ni_4(H_2chdp)(Hchdp)]\}^+$ species having m/z = 1119. Therefore, the mass spectrometric results suggest that the tetrameric forms of all the three complexes are stable in solution.

Potentiometric titrations

Potentiometric titrations of all the complexes were performed to determine the pK_a values of the coordinated water molecules in MeOH-H_2O (1:1; v/v); the ionic strength was maintained at $I = 0.1$ M $NaClO_4$. The curves obtained from the titration of complexes **1**, **2** and **3** with NaOH are shown in Figs. 5, S13 and S14. The titration results indicate that the neutralization occurs with 2 mol of NaOH per mol of each complex in the pH range of 6-12. Two deprotonation constants have been evaluated for each complex by treating the potentiometric titration data. The pK_a values of the coordinated water molecules were calculated to be 8.15 and 9.94 for **1**, 7.98 and 8.42 for **2**, and 8.34 and 10.32 for **3**. These pK_a values are more or less comparable to the value obtained for nickel(II)-bound water (cf. the pK_a of $[Ni(H_2O)_6]^{2+}$ is approximately 9.9).[46] The representative species distribution curves for complexes **1** and **3** are shown in Figs. 6 and S15. The species distribution curves show that all the three complexes exist predominantly in their corresponding tetrameric species in solution, in the pH range of 6-12. From the potentiometric titration results, we are prone to believe that the two pK_a values observed for each complex are due to the conversion of "$Ni^{II}_2(H_2O)_2$-$Ni^{II}_2(H_2O)_2$" to "$Ni^{II}_2(H_2O)_2$-$Ni^{II}_2(H_2O)(OH)$" species (pK_{a1}) and "$Ni^{II}_2(H_2O)_2$-$Ni^{II}_2(H_2O)(OH)$" to "$Ni^{II}_2(H_2O)(OH)$-$Ni^{II}_2(H_2O)(OH)$" species (pK_{a2}) (Scheme 4). Therefore, in essence, we have proposed the formation of the species "$Ni^{II}_2(H_2O)(OH)$-$Ni^{II}_2(H_2O)(OH)$" as the active species during phosphoester hydrolysis.

Phosphoester hydrolysis

In order to evaluate the phosphatase-like activity[47-50] of complexes **1**, **2** and **3**, the hydrolysis of bis(*p*-nitrophenyl) phosphate (BNPP) was examined in methanol-water (1:1; v/v) solution at pH~10.5 and 11.8. Each of these complexes are suitable candidates for the catalytic hydrolysis, as it is observed to possess loosely bound water molecules where suitable substrates may bind. The hydrolysis experiments have been carried out spectrophotometrically by monitoring the increase in absorption band of the liberated *p*-nitrophenolate anion at 400 nm under the pseudo-first-order reaction conditions.

       In the first set of experiments, the pH dependence of catalytic activities of the complexes was investigated in the pH range of 8.0-12.5 at 30°C. As shown in Fig. 7, the

rate versus pH plots for all the three complexes have sigmoidal shapes, characteristic of a kinetic process controlled by an acid-base equilibrium. The experimental data reveal that the rate is highly influenced by the pH of solution, the reaction rate increases with increase in pH, and finally gets saturated above pH~11.8.

The kinetics data of hydrolysis of BNPP were obtained using initial rate method by monitoring the increase of p-nitrophenolate band at 400 nm as a function of time, keeping the substrate concentration at least 10 times larger than that of the catalyst to maintain the pseudo-first-order reaction conditions. The dependence of the initial rate on complex and substrate concentrations was examined in order to elucidate the reactivity. The kinetics data reveal that for all the three complexes the rate of hydrolysis is linearly dependent on the concentration of complexes at both the pH~10.5 and 11.8 (Fig. 8). Again, keeping the pseudo-first-order reaction conditions (excess complex concentration), the following second-order rate constants (k_2) were calculated from the slope of the straight lines of k_{obs} versus complex concentration plots (Fig. 9): $k_2 = 0.11$ and 0.14 $M^{-1}s^{-1}$ for **1**, $k_2 = 0.19$ and 0.26 $M^{-1}s^{-1}$ for **2**, and $k_2 = 0.05$ and 0.09 $M^{-1}s^{-1}$ for **3**, at pH~10.5 and 11.8, respectively.

The dependence of rate on the substrate concentration and various kinetic parameters were evaluated by treating the solution of each complex with different concentrations of the substrate under aerobic conditions at pH~10.5 and 11.8. For all the complexes, a first-order dependence on the substrate concentration was observed at lower concentration of substrate and the saturation kinetics were observed at higher concentration of substrate. Applying the Michaelis-Menten approach of enzyme kinetics and using the equation $1/V = (K_m/V_{max}) (1/[S]) + 1/V_{max}$, we have obtained the Lineweaver-Burk (double reciprocal) plots and the values of various kinetic parameters k_{cat}, K_m, V_{max}, k_{cat}/K_m and k_{cat}/k_{uncat} (Table 1) at pH~10.5 and 11.8. The rate versus substrate concentration plots and the Lineweaver-Burk plots for the complexes are shown in Figs. 10, 11, 12, S16, S17 and S18. The turnover rates (k_{cat}) for complexes **1**, **2** and **3** are 1.68 x 10^{-5}, 2.26 x 10^{-5} and 1.18 x 10^{-5} s^{-1} at pH~10.5, and 7.51 x 10^{-5}, 14.42 x 10^{-5} and 2.68 x 10^{-5} s^{-1} at pH~11.8, respectively. From these k_{cat} values, it can be believed that the catalytic activities of the complexes are significantly higher at pH~11.8 than that at pH~10.5. The potentiometric titration results and the corresponding species distribution

curves reveal that the species which is mostly present and stable at pH~10.5 and 11.8, in solution, is [$Ni_4(H_2chdp)_2(H_2O)_2(OH)_2$]. The higher catalytic activities at pH~11.8 compared to that at pH~10.5, could be due to the two reasons: (i) the effective concentration of the active tetranickel(II) species [$Ni_4(H_2chdp)_2(H_2O)_2(OH)_2$] at pH~11.8, in solution, is higher than that at pH~10.5, as revealed by the species distribution curves, and (ii) the formation of strong hydrogen bond with the complexes exhibiting higher affinities toward the BNPP substrate is more facilitated at pH~11.8 compared to that at pH~10.5.

Furthermore, these k_{cat} values also indicate that the catalytic activities of complexes **1**, **2** and **3** are comparable to some reported dimetallic nickel(II)[17,40,51], zinc(II)[52,53] and iron(III)-zinc(II)[54] model complexes, but are quite lower than those reported by others.[55,56] It is also important to note that complex **2** is more reactive than complex **1**, followed by the complex **3** (Table 1). As expected, for any complex to act as an efficient catalyst for hydrolysis of the substrate, the incoming substrate should first get bound successfully to the catalyst, which is generally directed by a combination of geometrical and electronic factors of the metal-ligand complex. This occurrence should be followed by the attack of the metal-coordinated hydroxide to the substrate. In our present study, the different ability of complexes **1**, **2** and **3** to hydrolyze BNPP could be most possibly due to the difference in effective concentrations of the active tetranickel(II) species [$Ni_4(H_2chdp)_2(H_2O)_2(OH)_2$] in solution in the pH range of 10.5-11.8, as revealed by the species distribution curves. Therefore, the higher catalytic efficiency of **2** compared to **1** and **3** toward BNPP hydrolysis could be due to the higher effective concentration of the active species, in solution.

The hydrolysis of bis(*p*-nitrophenyl) phosphate (BNPP) in methanol-water (1:1; v/v) solution under the similar experimental conditions but in the absence of any catalyst has been executed. Therefore, an acceleration (k_{cat}/k_{uncat}) of BNPP hydrolysis has been calculated. All the three complexes are capable of cleaving the phosphoester bond in BNPP with an average acceleration of hydrolysis up to 1.82 x 10^2 fold at pH~10.5 and 3.69 x 10^2 fold at pH~11.8 over the background reaction. Again, the control experiments have been performed under similar experimental conditions to examine the hydrolysis of BNPP using free metal salts $NiCl_2 \cdot 6H_2O$ and $Ni(ClO_4)_2 \cdot 6H_2O$. As expected, the

hydrolysis of BNPP is not promoted by these free metal salts in solution, because most possibly a precipitate of $Ni(OH)_2$ is formed at such higher pH.

In recent years, a number of investigations have been performed to test the potential of dinickel(II) complexes with vacant labile coordination site(s) for the hydrolysis of phosphate esters.[41,49,50] The proposed mechanism for the hydrolysis of bis(p-nitrophenyl) phosphate (BNPP) by complexes **1**, **2** and **3** is given in Scheme 5, based on the results obtained from mass spectrometric, potentiometric titration and kinetic analyses. The potentiometric titration results indicate that the possible active species responsible for the catalytic hydrolysis is $[Ni_4(H_2chdp)_2(H_2O)_2(OH)_2]$. These results also show that the nickel(II)-bound hydroxide plays a crucial role in this catalysis reaction within the specified experimental conditions. In the proposed mechanism, it has been suggested that during the catalytic hydrolysis the substrate preferably binds as nucleophile with one nickel(II) center of an intra-dinuclear $[Ni^{II}_2]$ unit in the active species of the complexes. Then, the nickel(II)-bound hydroxide of the same intra-dinuclear $[Ni^{II}_2]$ unit undergoes a nucleophilic attack to the phosphorous atom of the substrate resulting in the formation of free phosphate and p-nitrophenolate ions in solution. Similar binding-cum-hydrolytic events of bis(p-nitrophenyl) phosphate with dinuclear nickel(II) and zinc(II) complexes have been reported in the literature.[51,57]

Conclusion

In conclusion, the present study unveils the results on the synthesis, structure, spectroscopic characterization and evaluation of catalytic phosphoester hydrolysis of three new tetranuclear $[Ni^{II}_2]_2$ complexes. The metallic cores of complexes **1** and **3** consist of four distorted octahedral nickel(II) ions with intra-ligand Ni---Ni separation of 3.527(7) Å and 3.507(1) Å, respectively. The complexes show a rare $\mu_3:\eta^2:\eta^1:\eta^1$ bridging mode of two benzoate groups of H_2chdp^{3-} ligands with each bridging among three nickel(II) ions. The complexes maintain the average intra-ligand nickel-nickel separation of 3.517 Å, which is the optimum cooperativity between two nickel centers for mimicking the structural and functional models to the active site of phosphorester hydrolases. In a simulated metal-metal distance and NO_5 coordination environment, all the three complexes exhibit moderate catalytic activity toward the phosphoester

hydrolysis. The catalytic efficiency of all the complexes is comparable toward the hydrolysis of bis(p-nitrophenyl) phosphate. The present investigation will positively provide the valuable insights and directions for the future design of hydrolytically active polynuclear transition metal complexes.

Experimental section

Synthesis of   N,N′-Bis[2-carboxybenzomethyl]-N,N′-Bis[hydroxyethyl]-1,3-diaminopropan-2-ol, H₅chdp. A solution of 2-carboxybenzaldehyde (4.643 g, 30.00 mmol) and NaOH (1.200 g, 30.00 mmol) in 100 ml methanol was added to 1,3-diamino-propan-2-ol (1.424 g, 15.00 mmol) in 20 ml methanol. The yellowish solution obtained was heated to 60°C while stirring for ~ 4 h. Then, the solution was cooled in an ice-bath. Excess NaBH₄ (1.500 g, 39.50 mmol) was added in portions to the cold solution while stirring. The yellow color was slightly discharged. After 30 min, 2 ml conc. HCl was added drop wise to destroy the excess NaBH₄. Acidification of the solution to pH ~ 5 by the addition of more conc. HCl resulted in the precipitation of a white crystalline solid. The white solid was filtered, washed with H₂O and methanol, and dried at ~ 80°C. Yield: 4.95 g (87%). The compound was recrystallized from warm MeOH-H₂O (1:1; v/v) solution and confirmed by the elemental analysis as **H₃cdp·H₂O**. Anal. Calcd. for C₁₉H₂₂N₂O₅·H₂O: C, 60.63%; H, 6.43%; N, 7.44%. Found: C, 60.25%; H, 6.28%; N, 7.33%. ¹H NMR for the sodium salt of the compound (400 MHz, D₂O, 25°C, δ): 7.46-7.32 (m, 8H), 3.92- 3.80 (m, 1H), 2.63 (q, 4H), 2.55 (q, 4H).

A solution of 2-iodoethanol (2.145g, 12.50 mmol) in 10 ml water was added drop wise to a solution of N,N′-Bis(2-carboxybenzomethyl)-1,3-diaminopropan-2-ol, **H₃cdp** (1.790 g, 5.00 mmol) and NaOH (0.400 g, 10.00 mmol) in 25 ml water. The reaction mixture was refluxed for ~ 4 h. While refluxing, more NaOH (0.400 g, 10.00 mmol) was added in portions to maintain the pH ~11. The resulting solution was cooled and acidified with conc. HCl to pH ~5. The solution was then evaporated to dryness under vacuum to isolate an off-white solid product which was washed with acetone. The product was then extracted with dry methanol to discard the undesired salts and the methanol extract was evaporated to obtain an oily product. The oily product was triturated with 60-120 mesh

silica gel and was subjected to column chromatography using $CHCl_3$-MeOH (10:1; v/v) after washing the column by glacial acetic acid for 3-4 times. The product was re-crystallized as an off-white solid from MeOH-H_2O (1:1; v/v) solution to make it free from acetic acid. The product was confirmed by the elemental analysis, FTIR, ^1H and ^{13}C NMR, and mass spectrometry. Anal. Calcd. for $C_{23}H_{30}N_2O_7$: C, 61.87%; H, 6.77%; N, 6.27%. Found: C, 61.75%; H, 6.86%; N, 6.14%. FTIR (cm^{-1}): ν = 3452(b), 1651(s), 1590(s), 1562(s), 1475(s), 1457(s) 1399(s), 1307(s), 1214(s), 1154(s), 1091(s), 868(s), 740(s). ^1H NMR (400 MHz, D_2O, room temperature, δ): 7.47-7.50 (m, 2H), 7.34-7.41 (m, 6H), 3.98 (d, 2H), 3.79-3.86 (m, 3H), 3.59-3.65 (m, 4H), 2.72-2.80 (m, 4H), 2.64 (d, 2H), 2.47-2.52 (m, 2H). ^{13}C NMR (100 MHz, D_2O, room temperature, δ): 177.89, 139.61, 133.00, 131.18, 129.06, 128.12, 127.57, 64.86, 57.93, 57.64, 57.57, 55.68. Mass spectrum (ESI): m/z 507 (M^+ = {H_5chdp·$3H_2O$+Li}$^+$).

Synthesis of [Ni$_4$(H$_2$chdp)$_2$(H$_2$O)$_4$]Br$_2$·4CH$_3$OH·3H$_2$O (1). A methanol (10 ml) solution of $NiCl_2$·$6H_2O$ (0.266 g, 1.12 mmol) was added to a solution of H_5chdp (0.250 g, 0.56 mmol) and NaOH (0.067g, 1.68 mmol) in methanol (10 ml) with magnetic stirring during a period of 10 min. The reaction mixture was then stirred for 2 h resulting in a light green solution. The solution was filtered to discard any insoluble precipitate. Then, 2 ml aqueous solution of NaBr (0.058 g, 0.56 mmol) was added drop wise and the reaction mixture was stirred for another 1 h. The solution was filtered again to discard any insoluble precipitate. The X-ray quality green plate shaped single crystals were obtained by slow ether diffusion into the clear filtrate after ~ 15 days. Yield: 0.298 g (75%). Anal. Calcd for $C_{47}H_{69}N_4O_{20.5}Br_2Ni_4$ (**1**-$3CH_3OH$·$1.5H_2O$): C, 39.96; H, 4.92; N, 3.97; Ni, 16.62; Found: C, 40.74; H, 4.98; N, 4.02; Ni, 16.49. FTIR (KBr, cm^{-1}): ν = 3412(b), 1631(s), 1586(s), 1559(s), 1454(s), 1386(s), 1365(s), 1155(s), 1121(s), 1045(s), 995(s), 963(s), 762(s), 672(s). UV-Vis (MeOH-H_2O): λ_{max} (ε, $M^{-1}cm^{-1}$) = 683 (138), 276 (1391), 220 (6971). Mass spectrum (ESI): m/z 1119 (M^+ = {[Ni$_4$(H$_2$chdp)(Hchdp)}$^+$), 560 (M^+ = {[Ni$_4$(H$_2$chdp)(Hchdp)}$^{2+}$).

Synthesis of [Ni$_4$(H$_2$chdp)$_2$(H$_2$O)$_4$](PF$_6$)$_2$ (2). This compound was prepared as microcrystalline powder following the above procedure using $NiCl_2$·$6H_2O$, NaOH and

NH$_4$PF$_6$. Yield: 0.307 g (71%). Anal. Calcd for C$_{48}$H$_{70}$N$_4$O$_{20}$P$_2$F$_{12}$Ni$_4$ (**2**·2CH$_3$OH): C, 37.25; H, 4.56; N, 3.62; Ni, 15.17; Found: C, 37.04; H, 4.39; N, 3.56; Ni, 15.55. FTIR (KBr, cm^{-1}): ν = 3392(b), 1629(s), 1593(s), 1548(s), 1465(s), 1404(s), 1340(s), 1212(s), 1159(s), 1105(s), 854(s), 845(b), 762(s), 590(s), 565(s). UV-Vis (MeOH-H$_2$O): λ_{max} (ε, M^{-1}cm^{-1}) = 685 (146), 277 (1430), 223 (7530). Mass spectrum (ESI): m/z 1119 (M^+ = {[Ni$_4$(H$_2$chdp)(Hchdp)}$^+$), 560 (M^+ = {[Ni$_4$(H$_2$chdp)(Hchdp)}$^{2+}$).

Synthesis of [Ni$_4$(H$_2$chdp)$_2$(H$_2$O)$_4$](ClO$_4$)$_2$·3.2CH$_3$OH·0.8H$_2$O (3). This compound was prepared following the above procedure using Ni(ClO$_4$)$_2$·6H$_2$O and NaOH. The X-ray quality green block shaped single crystals were obtained by slow evaporation of the clear filtrate after ~ 10 days. Yield: 0.281 g (71%). Anal. Calcd for C$_{47}$H$_{66}$N$_4$O$_{27}$Cl$_2$Ni$_4$ (**3**-2.2CH$_3$OH·0.8H$_2$O): C, 39.62; H, 4.67; N, 3.93; Ni, 16.48; Found: C, 39.78; H, 4.67; N, 3.91; Ni, 16.49. FTIR (KBr, cm^{-1}): ν = 3435(b), 1630(s), 1589(s), 1555(s), 1451(s), 1401(s), 1368(s), 1089(s), 941(s), 897(s), 759(s), 636(s), 627(s). UV-Vis (MeOH-H$_2$O): λ_{max} (ε, M^{-1}cm^{-1}) = 658 (154), 279 nm (ε, 1285 M^{-1}cm^{-1}) and 225 nm (ε, 6529 M^{-1}cm^{-1}). Mass spectrum (ESI): m/z 1119 (M^+ = {[Ni$_4$(H$_2$chdp)(Hchdp)}$^+$), 560 (M^+ = {[Ni$_4$(H$_2$chdp)(Hchdp)}$^{2+}$).

Caution

Perchlorate salts of metal complexes are potentially explosive and should be handled in small quantities with great care.

Materials

2-Carboxybenzaldehyde, 1,3-diamino-2-propanol, iodoethanol, bis(*p*-nitrophenyl) phosphate and ammonium hexafluorophosphate were purchased from Sigma-Aldrich Chemie GmbH, Germany. Nickel(II) chloride hexahydrate, sodium hydroxide and sodium bromide were purchased from Merck, India. CAPS buffer was purchased from SRL, India. Nickel(II) perchlorate hexahydrate was prepared by treating nickel(II) carbonate with 1:1 perchloric acid and crystallized after concentrating on water bath. All other chemicals and solvents were reagent grade materials and were used as received from commercial sources without further purification.

14

Physical measurements

Microanalyses (C,H,N) were performed using a Perkin-Elmer 2400 CHNS/O Series II elemental analyzer. FTIR spectra were obtained on a Perkin-Elmer L120-000A spectrometer (400-4000 cm^{-1}). ^{1}H and ^{13}C NMR spectra were obtained in D$_2$O solution on a Bruker AC 400 NMR spectrometer. ESI mass spectra were recorded using a Micromass Q-Tof Micro™ (Waters) mass spectrometer. UV-Vis spectra were recorded on a Shimadzu UV 1800 (190-1100 nm) (1 cm quartz cell) spectrophotometer.

Potentiometric measurements

Potentiometric titrations of the complexes were carried out at 30°C using a Mettler Toledo Seven Compact S220 digital Ion/pH meter in MeOH-H$_2$O (1:1; v/v) solution by adjusting the ionic strength to 0.1 M of NaClO$_4$. To balance the expected methanol-water liquid junction potential, a correction of pH value of ~ 0.051 units were subtracted from the measured pH readings.[58] Computations were performed with the HYPERQUAD 2000 program and species distribution curves were obtained using the program HySS.[59] To determine the pK_a values of the coordinated water molecules in complexes **1**, **2** and **3**, a typical pH-metric titration was executed as follows: 1 mM MeOH-H$_2$O (1:1; v/v) solutions of the complexes were titrated separately with 0.01 M NaOH solution. The ionic strength of the solution was maintained at $I = 0.1$ M of NaClO$_4$.

Kinetic measurements

Phosphatase-like activities of complexes **1**, **2** and **3** were determined through the hydrolysis reaction of the model substrate, bis(*p*-nitrophenyl) phosphate (BNPP) under pseudo first-order reaction conditions. The kinetic experiments were performed in 3 ml UV cells in MeOH-H$_2$O (1:1; v/v) solution. The solution was buffered using 20 mM CAPS buffer (pH~10.5 and 11.8). The ionic strength was maintained at $I = 0.1$ M NaClO$_4$. 1 mM stock solution of each complex was added separately in requisite amount to maintain the concentration of each complex at 0.25 mM in cuvette and 50 mM BNPP stock solution was added in requisite amounts to vary the concentrations from 5 mM to 25 mM in cuvette. Required amount of buffer was added to make up the volume. All the ingredients were mixed in a thermostatic cell (30°C), and the visual spectrum was

recorded at 400 nm, where the molar extinction coefficient for the hydrolysis product p-nitrophenolate is 18500 $M^{-1}cm^{-1}$.[60] The total amount of p-nitrophenol/phenolate was determined by using the pKa (7.15).[60]

X-ray crystallography and data analysis

Crystal data and refinement parameters for both the complexes **1** and **3** are summarized in Table 2. Selected bond distances and bond angles are given in Table 3. A green plate shaped single crystal of complex **1** with approximate dimensions of 0.39 x 0.24 x 0.16 mm and a green block shaped single crystal of complex **3** with approximate dimensions of 0.26 x 0.18 x 0.13 mm were selected for structural analysis. Intensity data for complex **1** were collected using a diffractometer with Bruker SMART CCD area detector[61] and graphite-monochromated Mo Kα radiation (λ = 0.71073 Å). Similarly, intensity data for complex **3** were collected using a diffractometer with SuperNova, Dual, Cu at zero, Eos area detector and graphite-monochromated Cu Kα radiation (λ = 1.54184 Å). For complex **1**, a total of 5331 data were measured with Miller indices h_{min} = -12, h_{max} = 12, k_{min} = -13, k_{max} = 13, l_{min} = -16, l_{max} = 16, in the range of 1.96 < θ < 24.78° using ω oscillation frames. The data were corrected for absorption by the multi-scan method[62] giving minimum and maximum transmission factors. The data were merged to form a set of 4388 independent reflections with R = 0.0356. The residual electron density is in the range of +1.015 to -0.478 e·$Å^{-3}$. For complex **3**, a total of 5032 data were recorded with Miller indices h_{min} = -19, h_{max} = 20, k_{min} = -20, k_{max} = 14, l_{min} = -19, l_{max} = 23, in the range of 5.02 < θ < 66.19° using ω oscillation frames. The data were corrected for absorption by the multi-scan method[62] giving minimum and maximum transmission factors. The data were merged to form a set of 4536 independent reflections with R = 0.0587. The residual electron density is in the range of +1.900 to -0.642 e·$Å^{-3}$. The structures were solved by direct methods using the software SIR-97,[63] and refined by full-matrix least-squares methods on F^2 using the program SHELXL[64] embedded in the routine Olex2.[65] Hydrogen atom positions were initially determined by geometry and refined by riding model. Non-hydrogen atoms were refined with anisotropic displacement parameters. All hydrogen atoms were generated at ideal positions (C-H, 0.96 Å) and fixed with isotropic thermal parameters.

RSC Advances Accepted Manuscript

Acknowledgements

Electronic supplementary information (ESI) available:

FTIR, ^{1}H and ^{13}C NMR, and mass spectra of the ligand H_5chdp. Representative FTIR, UV-Vis, ESI mass spectra, potentiometric titration plots, species distribution curves and kinetics plots of the complexes. CCDC reference numbers 1417838 and 1417839 for complexes **1** and **3**, respectively. For ESI and crystallographic data in CIF or other electronic format see DOI: 10.1039/……………………

Notes and References

1 C. Piguet, G. Bernardinelli and G. Hopfgartner, *Chem. Rev.*, 1997, **97**, 2005.

2 C. Piguet, M. Borkovec, J. Hamacek and K. Zeckert, *Coord. Chem. Rev.,* 2005, **249**, 705.

3 A. C. Rosenzweig, C. A. Frederick, S. J. Lippard and P. Nordlund, *Nature,* 1993, **366**, 537.

4 D. A. Whittington and S. J. Lippard, *J. Am. Chem. Soc.*, 2001, **123**, 827.

5 E. Jabri, M. B. Carr, R. P. Hausinger and P. A. Karplus, *Science,* 1995, **268**, 998.

6 C. Gerdemann, C. Eicken and B. Krebs, *Acc. Chem. Res.*, 2002, **35**, 183.

7 R. M. Buchanan, M. S. Mashuta, K. J. Oberhausen, J. F. Richardson, Q. Li and D. N. Hendrickson, *J. Am. Chem. Soc.,* 1989, **111**, 4497.

8 M. A. Halcrow and G. Christou, *Chem. Rev.,* 1994, **94**, 2421.

9 M. J. Maroney, G. Davidson, C. B. Allan and J. Figlar, *Struct. Bonding,* 1998, **92**, 1.

10 S. Ciurli, S. Benini, W. R. Rypniewski, K. S. Wilson, S. Miletti and S. Mangani,

Coord. Chem. Rev., 1999, **190-192**, 331.

11 A. F. Kolodziej, *Prog. Inorg. Chem.,* 1994, **41**, 493.

12 P. A. Karplus, M. A. Pearson and R. P. Hausinger, *Acc. Chem. Res.,* 1997, **30**, 330.

13 G. Brunet, F. Habib, C. Cook, T. Pathmalingam, F. Loiseau, I. Korobkov, T. J. Burchell, A. M. Beauchemin and M. Murugesu, *Chem. Commun.*, 2012, 1287.

14 G. Aromi, A. Bell, S. J. Teat and R. E. P. Winpenny, *Chem. Commun.,* 2005, 2927.

15 R. Biswas, S. Mukherjee, P. Kar and A. Ghosh, *Inorg. Chem.,* 2012, **51**, 8150.

16 A. K. Ghosh, M. Shatruk, V. Bertolasi, K. Pramanik and D. Ray, *Inorg. Chem.,* 2013, **52**, 13894.

17 H. Carlsson, M. Haukka, A. Bousseksou, J. M. Latour and E. Nordlander, *Inorg. Chem.*, 2004, **43**, 8252.

18 G. Aromi, O. Roubeau, M. Helliwell, S. J. Teat and R. E. P. Winpenny, *Dalton Trans.,* 2003, 3436.

19 M. Gustafsson, A. Fischer, A. Ilyukhin, M. Maliarik and P. Nordblad, *Inorg. Chem.,* 2010, **49**, 5359.

20 A. Bell, G. Aromi, S. J. Teat, W. Wernsdorfer and R. E. P. Winpenny, *Chem. Commun.*, 2005, 2808.

21 C. Papatriantafyllopou, G. Aromi, A. J. Tasiopoulos, V. Nastopoulos, C. P. Raptopoulou, S. J. Teat, A. Escuer and S. P. Perlepes, *Eur. J. Inorg. Chem.,* 2007, 2761.

22 A. R. Paital, W. T. Wong, G. Aromi and D. Ray, *Inorg. Chem.,* 2007, **46**, 5727.

23 D. Mandal, V. Bertolasi, G. Aromi and D. Ray, *Dalton Trans.,* 2007, 1989.

24 T. C. Stamatatos, K. A. Abboud, W. Wernsdorfer and G. Christou, *Angew. Chem., Int. Ed.*, 2007, **46**, 884.

25 M. Murugesu, R. Clerac, W. Wernsdorfer, C. E. Anson and A. K. Powell, *Angew. Chem., Int. Ed.*, 2005, **44**, 6678.

26 M. Bera, A. B. S. Curtiss, G. T. Musie and D. R. Powell, *Inorg. Chem.*, 2012, **51**, 12093.

27 A. Patra, T. K. Sen, A. Ghorai, G. T. Musie, S. K. Mandal, U. Ghosh and M. Bera, *Inorg. Chem.,* 2013, **52**, 2880.

28 C. D. Stewart, H. Arman, H. Bawazir and G. T. Musie, *Inorg. Chem.,* 2014, **53**,

10974.

29 A. Patra, S. K. Saha, T. K. Sen, L. Carrella, G. T. Musie, A. R. Khuda-Bukhsh and M. Bera, *Eur. J. Inorg. Chem.,* 2014, 5217.

30 S. Haldar, A. Patra and M. Bera, *RSC Adv.,* 2014, **4**, 62851.

31 A. B. S. Curtiss, M. Bera, G. T. Musie and D. R. Powell, *Dalton Trans*., 2008, 2717.

32 M. Bera, A. B. S. Curtiss, G. T. Musie and D. R. Powell, *Inorg. Chem. Commun*., 2008, **11**, 1033.

33 M. Bera, G. T. Musie and D. R. Powell, *Inorg. Chem. Commun*., 2010, **13**, 1029.

34 M. Bera, G. T. Musie and D. R. Powell, *Inorg. Chem.,* 2009, **48***,* 4625.

35 A. Patra, G. C. Giri, T. K. Sen, L. Carrella, S. K. Mandal and M. Bera, *Polyhedron,* 2014, **67**, 495.

36 R. C. Mehrotra and R. Bohra, *Metal Carboxylate*; Academic Press: New York, 1983.

37 R. L. Rardin, W. B. Tolman and S. J. Lippard, *New. J. Chem.,* 1991, **15**, 417.

38 (a) H. C. Freeman, F. Huq and G. N. Stephens, *J. Chem. Soc.*, *Chem. Commun.,* 1976, 90; (b) F. A. Cotton, G. E. Lewis and G. N. Mott, *Inorg. Chem.,* 1983, **22**, 1825; (c) W. Clegg, T. R. Little and B. P. Straughan, *Inorg. Chem.,* 1988, **27**, 1916.

39 K. B. Wiberg and K. E. Laidig, *J. Am. Chem. Soc.,* 1987, **109**, 5935.

40 S. Mandal, V. Balamurugan, F. Lloret and R. Mukherjee, *Inorg. Chem.,* 2009, **48**, 7544.

41 H. Carlsson, M. Haukka and E. Nordlander, *Inorg. Chem.,* 2002, **41**, 4981.

42 G. B. Deacon and R. J. Philllips, *Coord. Chem. Rev*., 1980, **33**, 227.

43 V. Zelenak, Z. Vargova and K. Gyoryova, *Spectrochim. Acta, Part A*, 2007, **66**, 262.

44 (a) J. Sletten, A. Sorensen, M. Julve and Y. Journaux, *Inorg. Chem*., 1990, **29**, 5054; (b) A. M. Heyns, *Spectrochim. Acta*, 1977, **33A**, 315.

45 B. J. Hathaway, G. Wilkinson, R. G. Gillard and J. A. McCleverty, Eds.; *Comprehensive Coordination Chemistry;* Pergamon: Oxford, 1987*,* **2***,* 413.

46 (a) A. M. Barrios and S. J. Lippard, *J. Am. Chem. Soc*., 1999, **121**, 11751; (b) D. W. Barnum, *Inorg. Chem*., 1983, **22**, 2297.

47 F. Mancin and P. Tecilla, *New J. Chem.,* 2007, **31**, 800.

48 J. R. Morrow and O. Iranzo, *Curr. Opin. Chem. Biol.,* 2004, **8**, 192.

49 D. Volkmer, B. Hommerich, K. Griesar, W. Haase and B. Krebs, *Inorg. Chem.,* 1996,

35, 3792.

50 A. Greatti, M. Scarpellini, R. A. Peralta, A. Casellato, A. J. Bortoluzzi, F. R. Xavier, R. Jovito, M. A. de Brito, B. Szpoganicz, Z. Tomkowicz, M. Rams, W. Haase and A. Neves, *Inorg. Chem.,* 2008, **47**, 1107.

51 C. Vichard and T. A. Kaden, *Inorg. Chim. Acta*, 2002, **337**, 173.

52 H. Arora, S. K. Barman, F. Lloret and R. Mukherjee, *Inorg. Chem*., 2012, **51**, 5539.

53 M. Jarenmark, E. Csapo, J. Singh, S. Wockel, E. Farkas, F. Meyer, M. Haukka and E. Nordlander, *Dalton Trans.*, 2010, **39**, 8183.

54 C. Piovezan, R. Jovito, A. J. Bortoluzzi, H. Terenzi, F. L. Fischer, P. C. Severino, C. T. Pich, G. G. Azzolini, R. A. Peralta, L. M. Rossi and A. Neves, *Inorg. Chem*. 2010, **49**, 2580.

55 B. de Souza, G. L. Kreft, T. Bortolotto, H. Terenzi, A. J. Bortoluzzi, E. E. Castellano, R. A. Peralta, J. B. Domingos and A. Neves, *Inorg. Chem*., 2013, **52**, 3594.

56 L. J. Daumann, G. Schenk, D. L. Ollis and L. R. Gahan, Lena, *Dalton Trans.*, 2014, **43**, 910.

57 S. Bosch, P. Comba, L. R. Gahan and G. Schenk, *Inorg. Chem.,* 2014, **53**, 9036.

58 R. G. Bates, M. Paabo and R. A. Robinson, *J. Phys. Chem*., 1963, **67**, 1833.

59 (a) P. Gans, A. Sabatini and A. Vacca, Talanta, 1996, **43**, 1739; (b) A. Alderighi, P. Gans, A. Ienco, D. Peters, A. Sabatini and A. Vacca, *Coord. Chem. Rev*. 1999, **184**, 311.

60 S. Albedyhl, M. T. Averbuch-Pouchot, C. Belle, B. Krebs, J. L. Pierre, E. Saint-Aman and S. Torelli, *Eur. J. Inorg. Chem.,* 2001, 1457.

61 (a) Data Collection: *SMART Software*, Bruker-AXS, 5465 E. Cheryl Parkway, Madison, WI 53711-5373 USA, 1998; (b) Data Reduction: *SAINT Software,* Bruker-AXS, 546E. Cheryl Parkway, Madison, WI 53711-5373 USA, 1998.

62 G. M. Sheldrick, *SADABS, Program for Multi-Scan Absorption Correction of Area Detector Data*, University of Göttingen, Germany, 2002.

63 C. Giacovazzo, A. Guagliardi, A. G. G. Moliterni, G. Polidori and R. Spagna, *J. Appl. Crystallogr.,* 1999, **32**, 115.

64 (a) G. M. Sheldrick, *SHELXTL*; Version 6.10 Reference Manual, Bruker-AXS, 5465

E. Cheryl Parkway, Madison, WI 53711-5373 USA, 2000; (b) *International Tables for Crystallography*, Vol C, Tables 6.1.1.4, 4.2.6.8, and 4.2.4.2, Kluwer: Boston, 1995.

65 O. V. Dolomanov, L. J. Bourhis, R. J. Gildea, J. A. K. Howard and H. Puschmann, *J. Appl. Cryst*. 2009, **42**, 339.
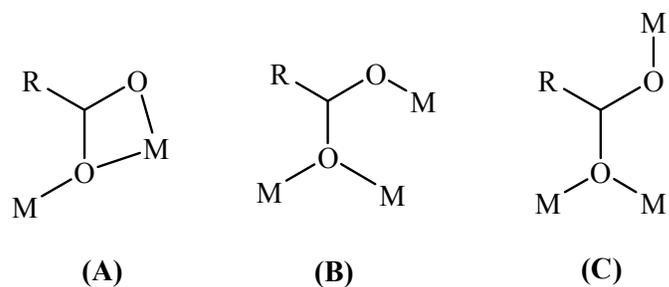
Schemes with Captions
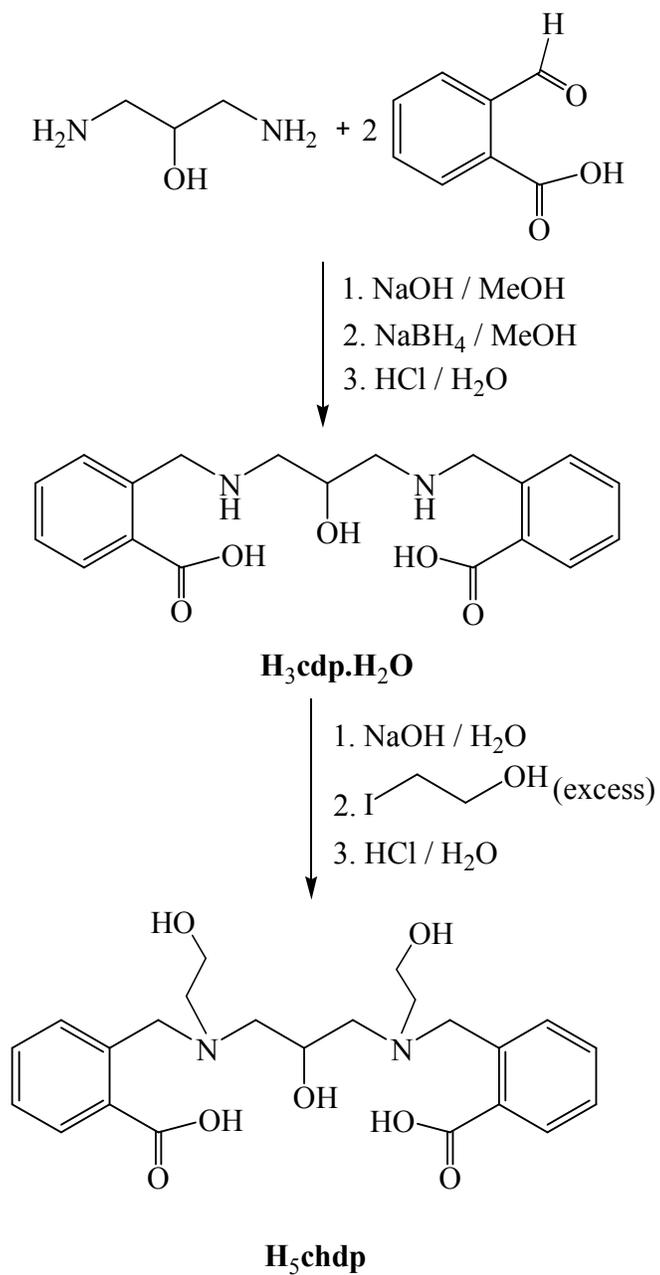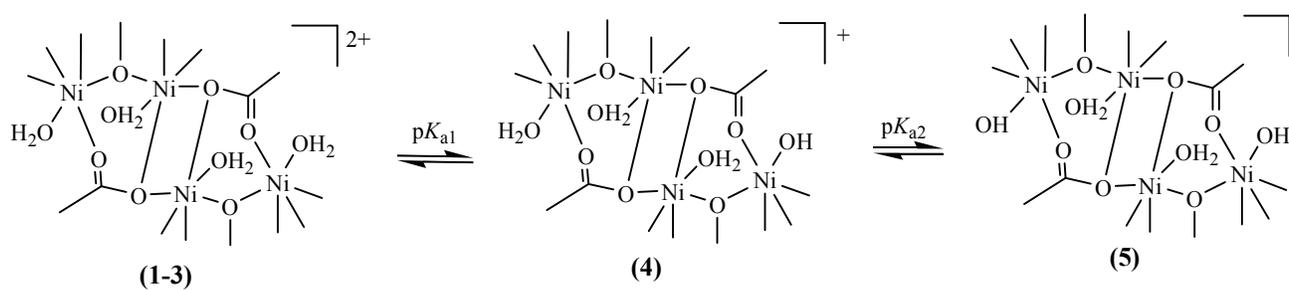

Scheme 1 Synthesis of the ligand, H$_5$chdp.
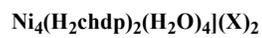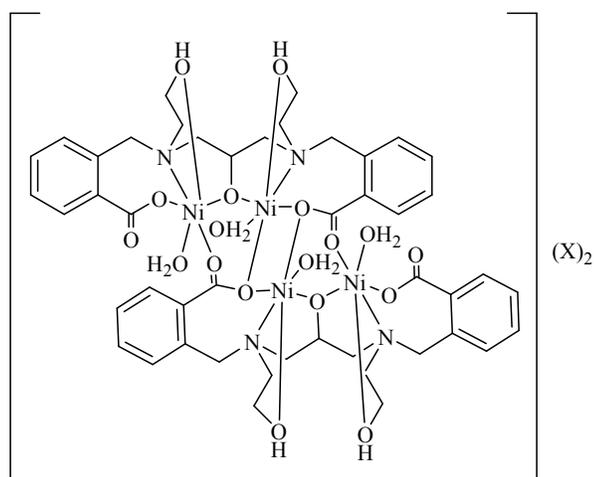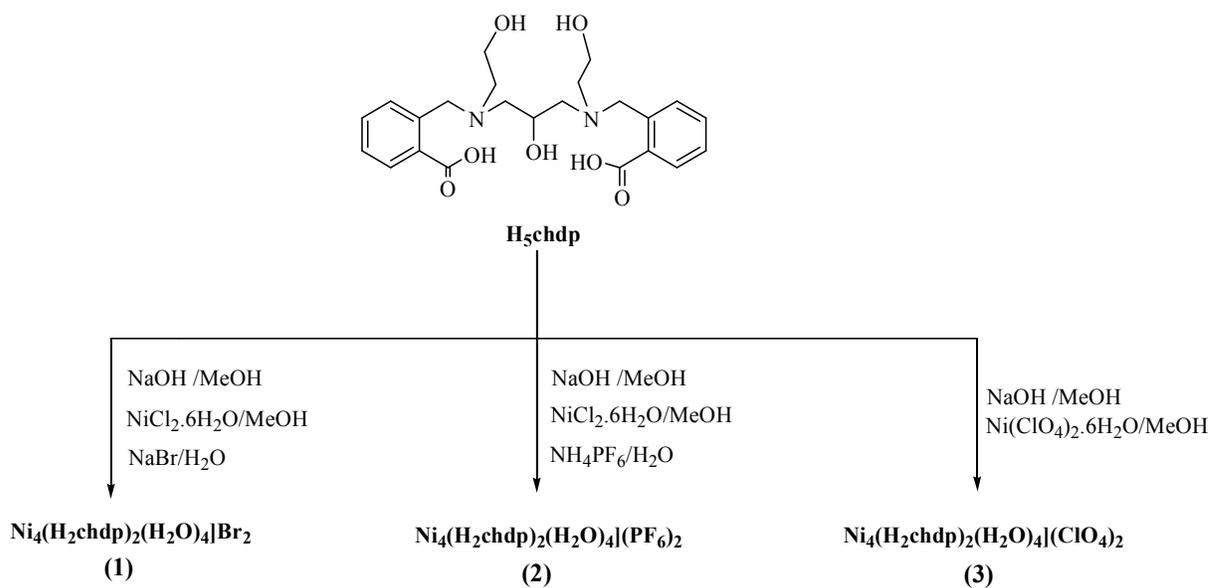
Scheme 2 Synthesis of the complexes.

Scheme 3 Binding modes of carboxylates in tridentate fashion.

Scheme 4 Conversion of the tetranuclear species of complexes **1**, **2** and **3** in MeOH-H_2O (1:1; v/v) solution.

Scheme 5 Proposed mechanism for the hydrolysis of BNPP by the complexes. Half part of each of the complexes is shown for clarity.

Figures with Captions
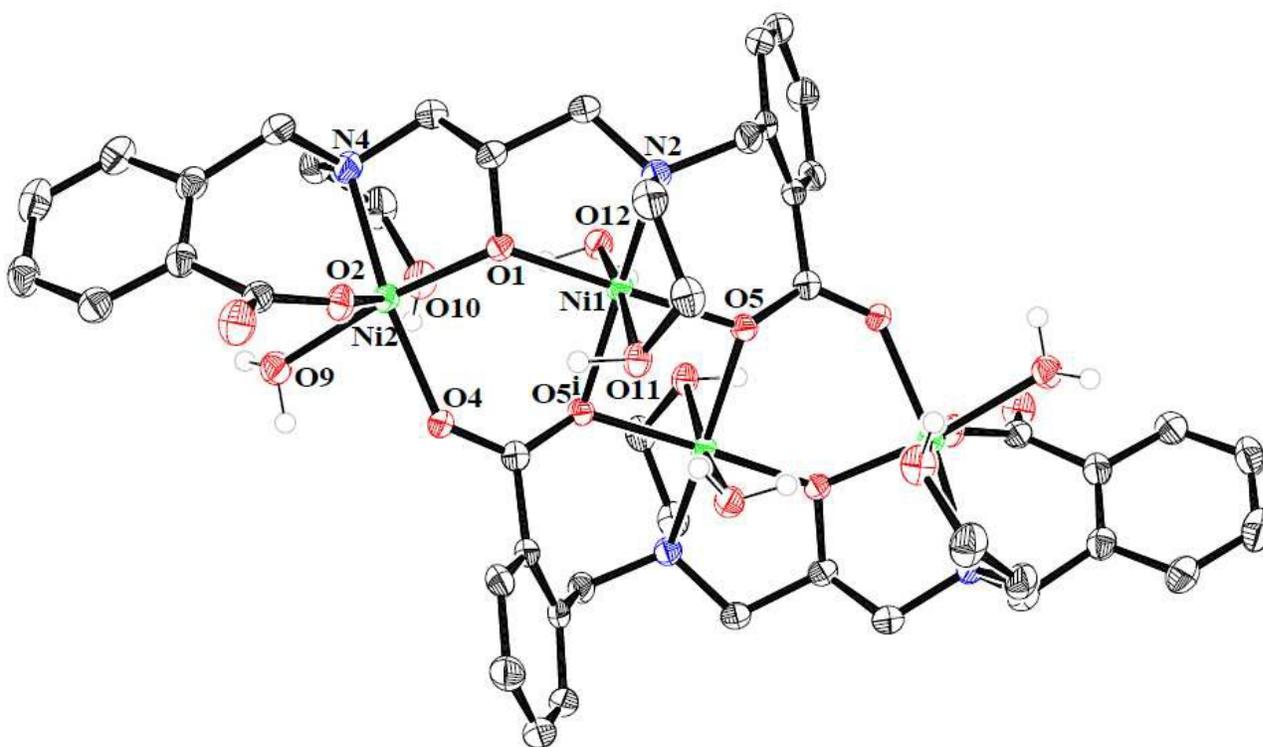
Fig. 1 Thermal ellipsoid (35%) plot of the molecular structure of complex [Ni$_4$(H$_2$chdp)$_2$(H$_2$O)$_4$]Br$_2$·4CH$_3$OH·3H$_2$O (**1**) with atom numbering scheme. Hydrogen atoms are omitted for clarity.
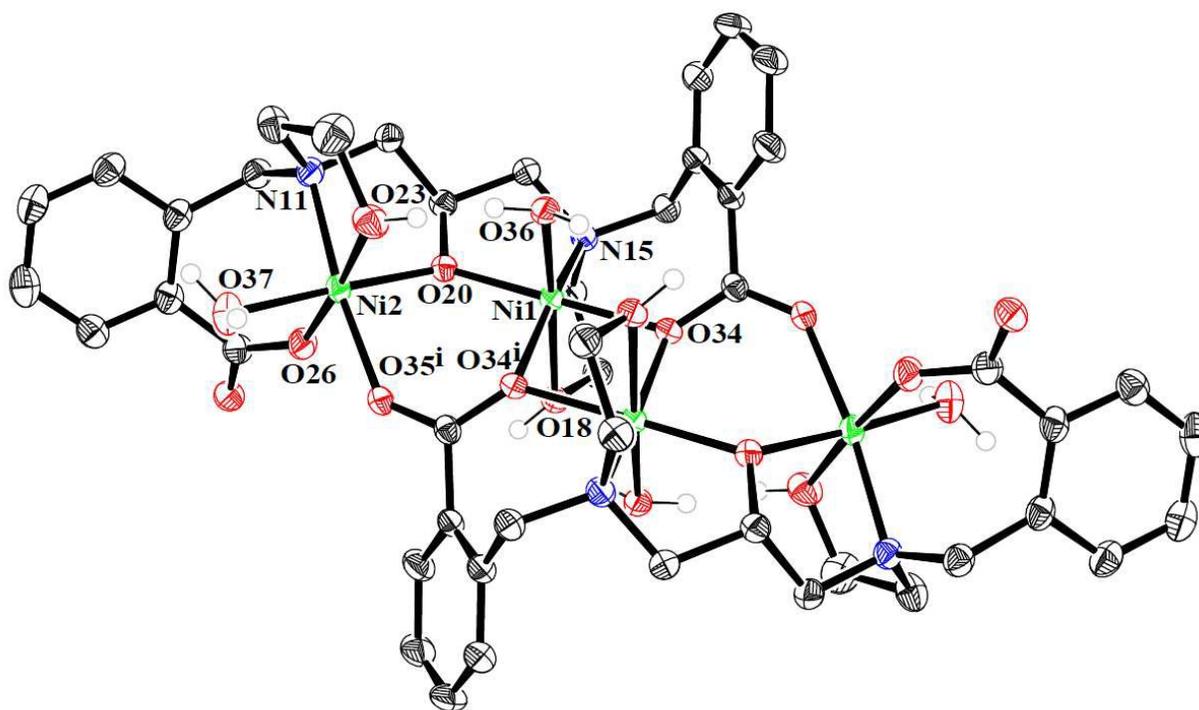
Fig. 2 Thermal ellipsoid (35%) plot of the molecular structure of complex [Ni$_4$(H$_2$chdp)$_2$(H$_2$O)$_4$](ClO$_4$)$_2 \cdot 3.2$CH$_3$OH$\cdot 0.8$H$_2$O (**3**) with atom numbering scheme. Hydrogen atoms are omitted for clarity.

Fig. 3 Thermal ellipsoid (35%) plot of the molecular structure of the dinuclear unit of complex **1** viewing the two aliphatic alcoholic arms of the ligand in *trans*-orientations.

Fig. 4 Thermal ellipsoid (35%) plot of the molecular structure of the dinuclear unit of complex **3** viewing the two aliphatic alcoholic arms of the ligand in *trans*-orientations.
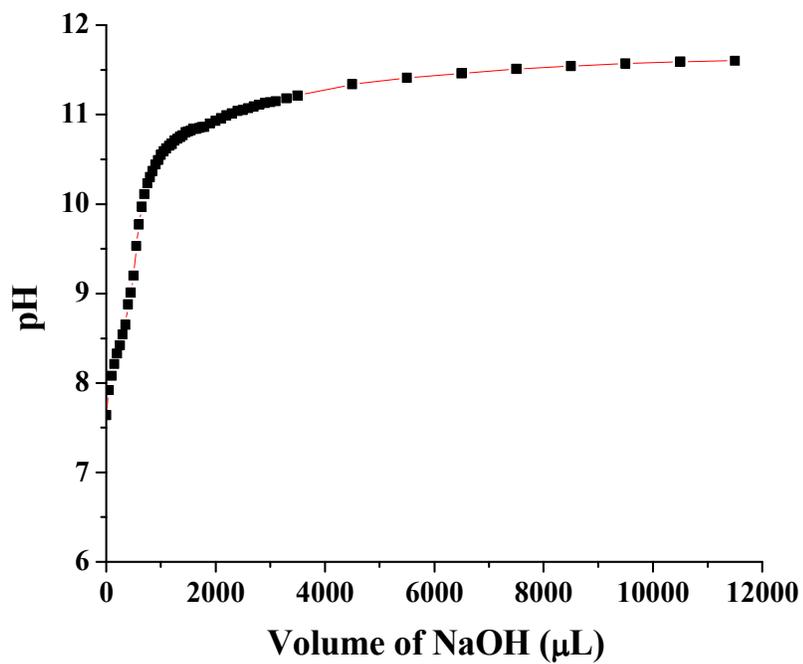
Fig. 5 Potentiometric titration curve obtained by titrating complex **1** with 0.01 M NaOH. The experimental points (black squares) are in good agreement with the theoretical curve (red line).
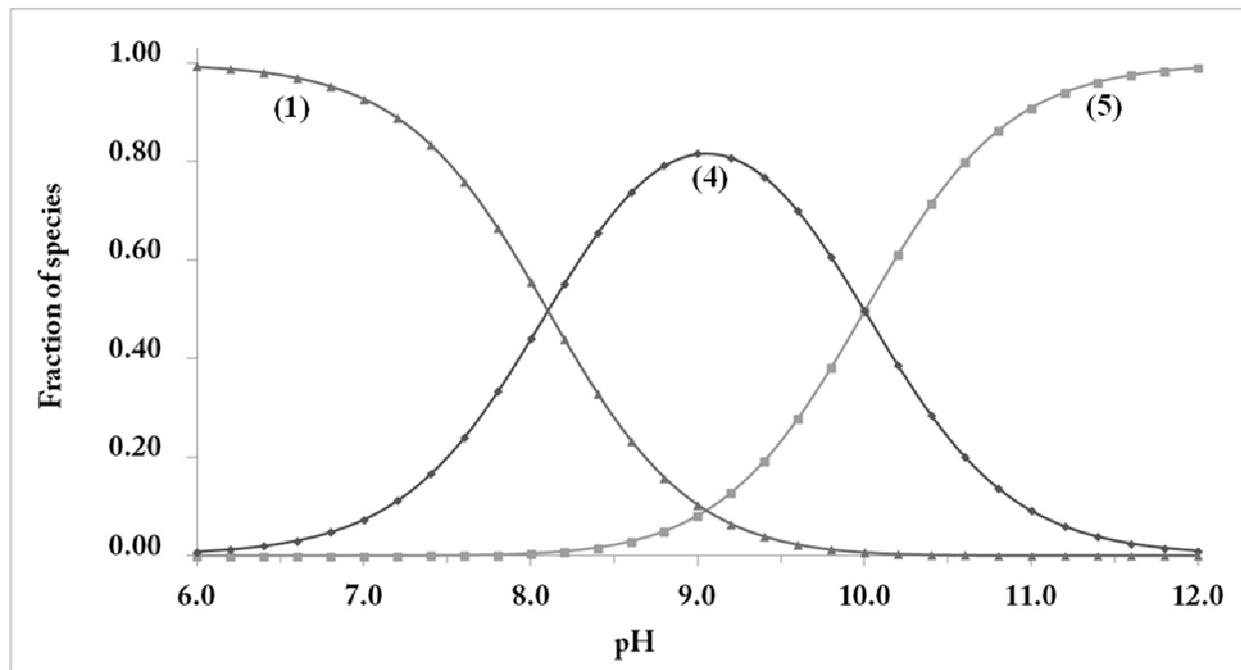
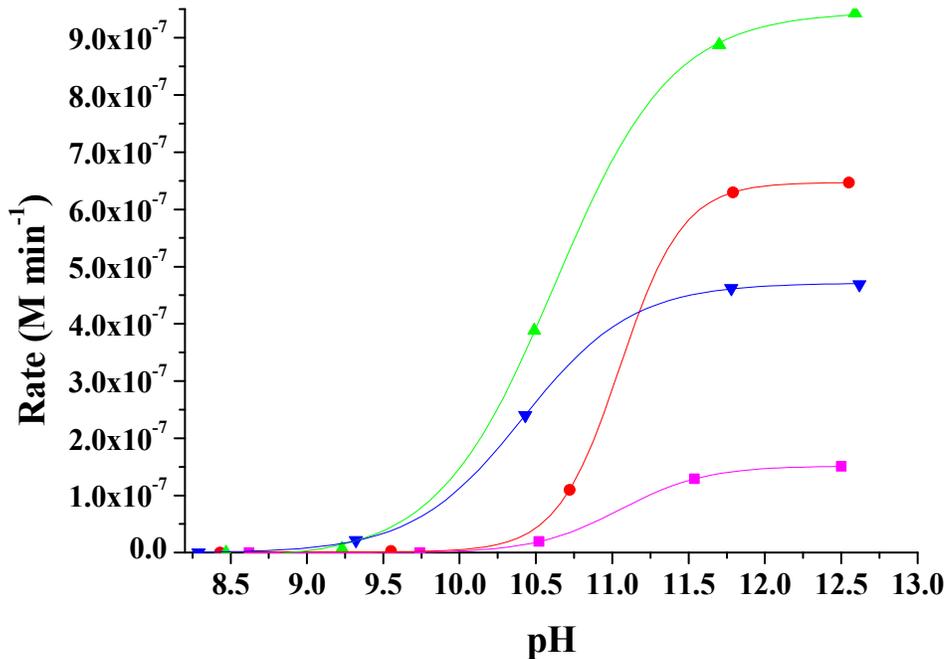**Fig. 6** Species distribution curves of complex **1** as a function of pH.

Fig. 7 Dependence of the rate on pH for the hydrolysis of BNPP in the absence of complex (■) and in the presence of complexes **1** (▼), **2** (▲) and **3** (●). [Complex] = 25 x 10^{-5} M; [BNPP] = 25 x 10^{-3} M; [Buffer] = 20 x 10^{-3} M; I = 0.1 M (NaClO$_4$) in MeOH-H$_2$O (1:1; v/v) at 30°C.
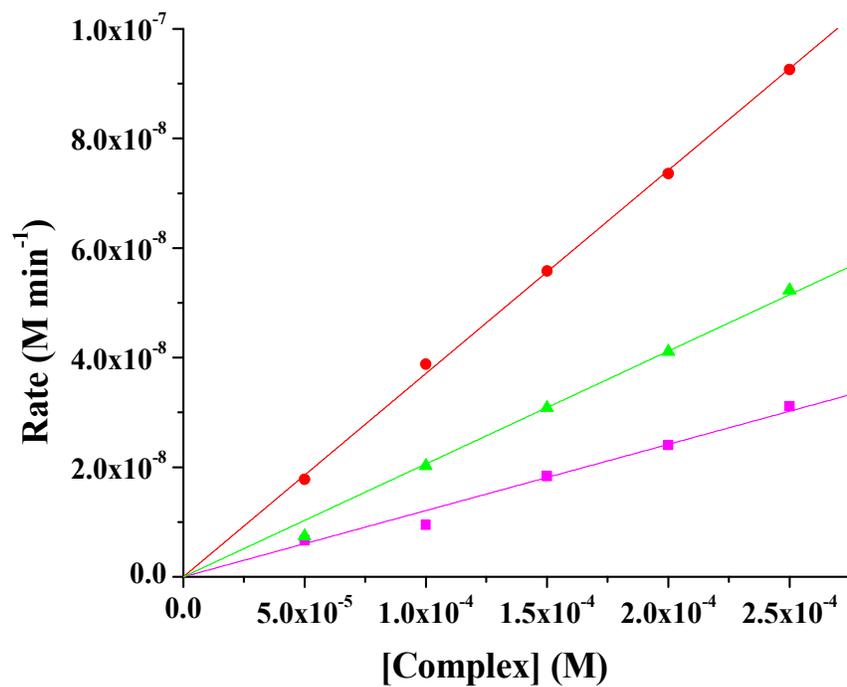
Fig. 8 Dependence of the rate on the concentration of complexes **1** (▲), **2** (●) and **3** (■) for the hydrolysis of BNPP. [BNPP] = 25 x 10^{-3} M; [Buffer] = 20 x 10^{-3} M; pH~10.5; I = 0.1 M (NaClO$_4$) in MeOH-H$_2$O (1:1; v/v) at 30°C.
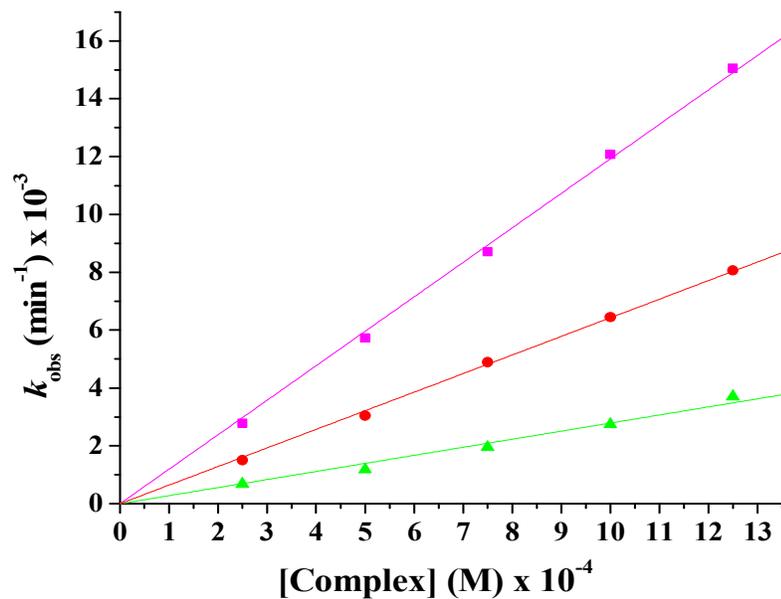
Fig. 9 Dependence of the observed rate constant (k_{obs}) on the concentration of complexes **1** (●), **2** (■) and **3** (▲) for the hydrolysis of BNPP. [BNPP] = 5 x 10^{-5} M; [Complex] = (25 - 125) x 10^{-5} M; [Buffer] = 20 x 10^{-3} M; pH~10.5; I = 0.1 M (NaClO$_4$) in MeOH-H$_2$O (1:1; v/v) at 30°C.

Fig. 10 Dependence of the rate on the concentration of substrate (BNPP) for complex **1**. Inset shows Lineweaver-Burk plot. [Complex] = 25 x 10^{-5} M; [Buffer] = 20 x 10^{-3} M; pH~10.5; I = 0.1 M (NaClO$_4$) in MeOH-H$_2$O (1:1; v/v) at 30°C.

Fig. 11 Dependence of the rate on the concentration of substrate (BNPP) for complex **2**. Inset shows Lineweaver-Burk plot. [Complex] = 25 x 10^{-5} M; [Buffer] = 20 x 10^{-3} M; pH~10.5; I = 0.1 M (NaClO$_4$) in MeOH-H$_2$O (1:1; v/v) at 30°C.

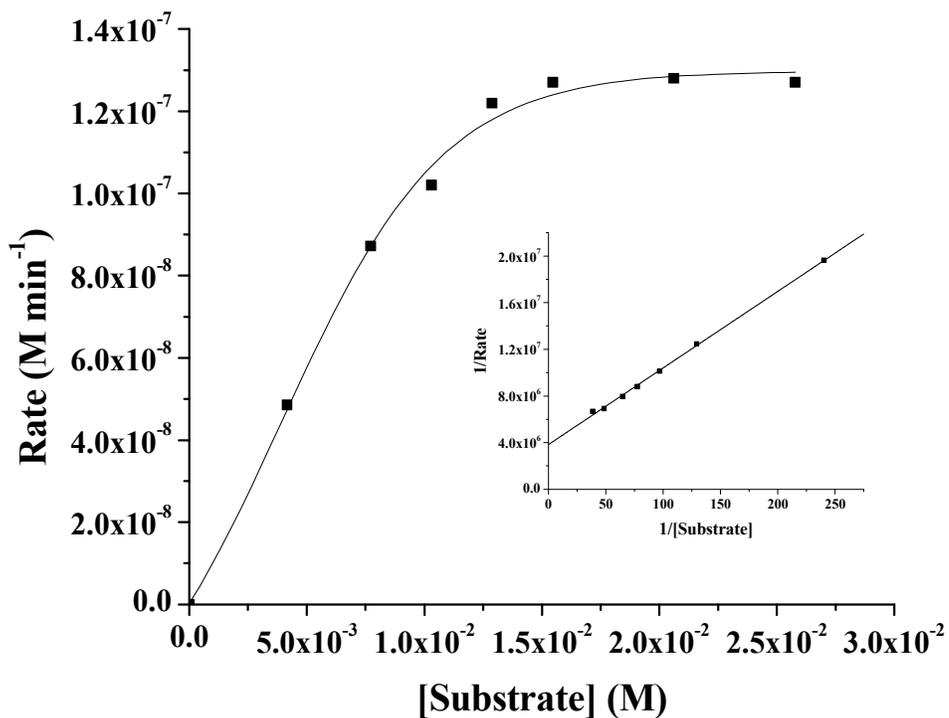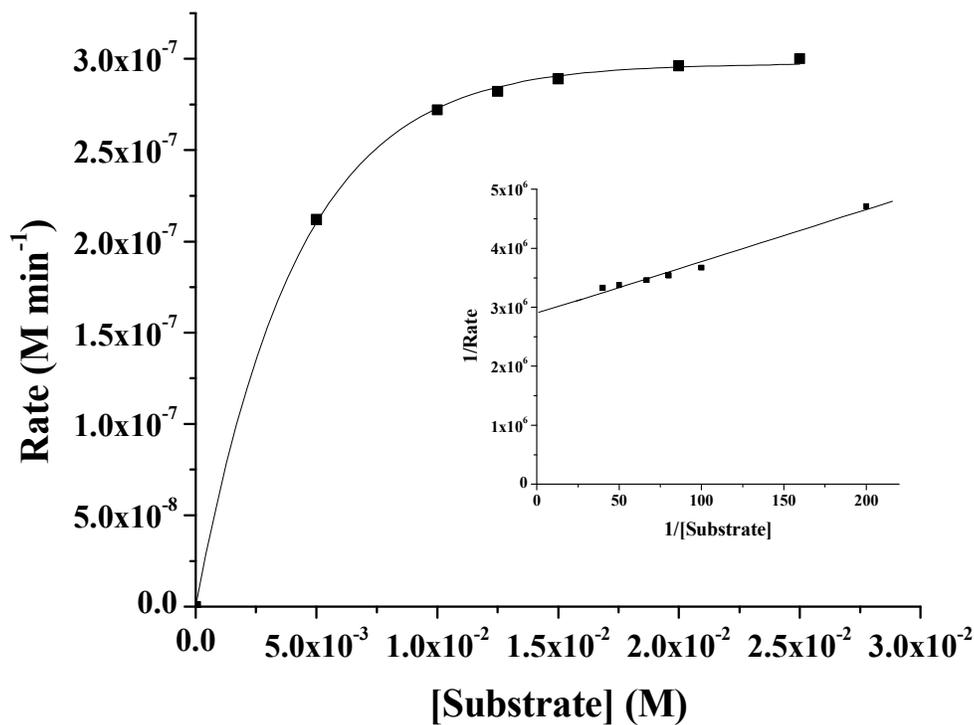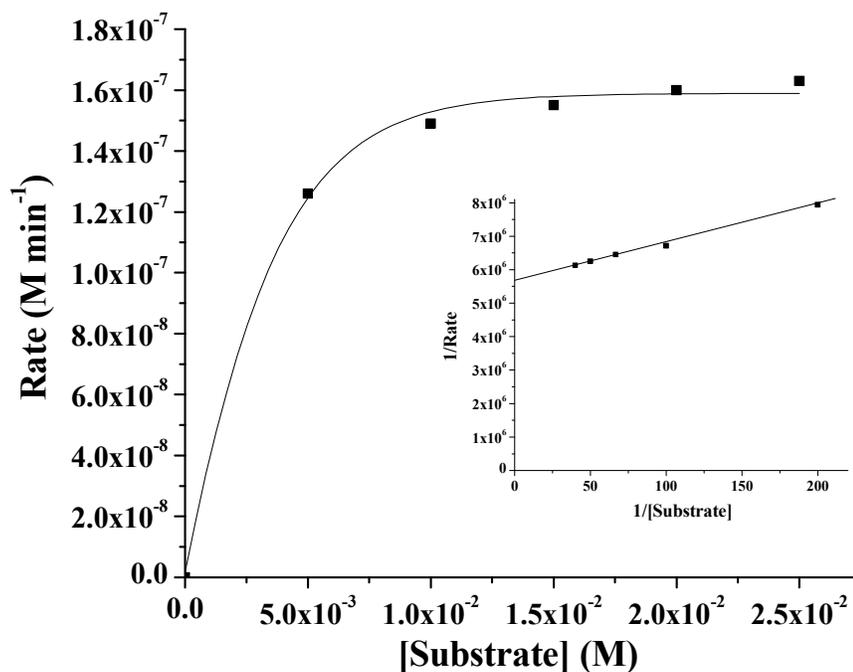**Fig. 12** Dependence of the rate on the concentration of substrate (BNPP) for complex **3**. Inset shows Lineweaver-Burk plot. [Complex] = 25 x 10^{-5} M; [Buffer] = 20 x 10^{-3} M; pH~10.5; I = 0.1 M (NaClO$_4$) in MeOH-H$_2$O (1:1; v/v) at 30°C.

Table 1 Kinetic parameters of complexes **1**, **2** and **3** for the hydrolysis of BNPP

Kinetic parameter	pH	1	2	3
k_{cat} (s^{-1})	10.5	1.68 x 10^{-5}	2.26 x 10^{-5}	1.18 x 10^{-5}
K_m (M)	10.5	2.66 x 10^{-3}	2.99 x 10^{-3}	1.98 x 10^{-3}
V_{max} (Ms^{-1})	10.5	4.20 x 10^{-9}	5.60 x 10^{-9}	2.94 x 10^{-9}
k_{cat}/K_m (M^{-1}s^{-1})	10.5	6.32 x 10^{-3}	7.55 x 10^{-3}	5.96 x 10^{-3}
k_{cat}/k_{uncat}	10.5	1.79 x 10^{2}	2.41 x 10^{2}	1.26 x 10^{2}
k_{cat} (s^{-1})	11.8	7.51 x 10^{-5}	14.42 x 10^{-5}	2.68 x 10^{-5}
K_m (M)	11.8	2.40 x 10^{-3}	18.09 x 10^{-3}	27.93 x 10^{-3}
V_{max} (Ms^{-1})	11.8	18.78 x 10^{-9}	36.05 x 10^{-9}	6.70 x 10^{-9}
k_{cat}/K_m (M^{-1}s^{-1})	11.8	31.2 x 10^{-3}	7.97 x 10^{-3}	0.95 x 10^{-3}
k_{cat}/k_{uncat}	11.8	3.38 x 10^{2}	6.49 x 10^{2}	1.20 x 10^{2}

Table 2 Crystal Data and Structure Refinement for Complexes **1** and **3**

	1	**3**
Empirical formula	$C_{50}H_{84}N_4O_{25}Br_2Ni_4$	$C_{49.2}H_{76.4}N_4O_{30}Cl_2Ni_4$
Formula weight	1535.87	1509.62
Crystal system	Triclinic	Orthorhombic
Space group	*P*-1	*Pbca*
a, Å	10.7231(14)	17.6138(3)
b, Å	11.7791(16)	17.4519(3)
c, Å	13.9580(19)	19.6556(5)
α, deg	109.907(2)	90.00
β, deg	93.565(3)	90.00
γ, deg	107.606(3)	90.00
Volume	1553.0(4)	6042.0(2)
Z	1	4
Density (calculated)	1.642 Mg/m^3	1.670 Mg/m^3
Wavelength	0.71073 Å	1.54184 Å
Temperature	273(2) K	293(2) K
F(000)	794	3160
Absorption coefficient	2.563 mm^{-1}	3.037 mm^{-1}
θ range for data collection	1.96 to 24.78°	5.02 to 66.19
Reflections collected	5331	5032
Independent reflections	4388	4536
R(*F* obsd data) [I > 2σ(I)]	0.0356	0.0587
wR(*F*^{2} all data)	0.0965	0.1609
Goodness-of-fit on *F*^{2}	1.051	1.046
Largest diff. peak and hole	+1.015 to –0.478 e/Å^3	+1.900 to -0.642 e/Å^3

$wR2 = \{ \Sigma \, [w(F_o{}^2 - F_c{}^2)^2] \, / \, \Sigma \, [w(F_o{}^2)^2] \,\}^{1/2}$

$R1 = \Sigma \, ||F_o| - |F_c|| \, / \, \Sigma \, |F_o|$

Table 3 Selected Bond Lengths [Å] and Angles [deg] in Complexes **1** and **3**

Bond Lengths [Å]

	(**1**)			(**3**)	
Ni(1)-O(1)	1.943(2)		Ni(1)-O(20)	1.955(3)	
Ni(1)-O(5)	2.058(2)		Ni(1)-O(34)	2.069(3)	
Ni(1)-N(2)	2.075(3)		Ni(1)-N(15)	2.079(4)	
Ni(1)-O(12)	2.105(3)		Ni(1)-O(36)	2.111(3)	
Ni(1)-O(11)	2.127(3)		Ni(1)-O(34^i)	2.120(3)	
Ni(1)-O(5^i)	2.131(2)		Ni(1)-O(18)	2.133(3)	
Ni(2)-O(1)	1.964(3)		Ni(2)-O(20)	1.957(3)	
Ni(2)-O(2)	2.032(3)		Ni(2)-O(26)	2.048(3)	
Ni(2)-O(4)	2.068(2)		Ni(2)-O(35^i)	2.070(3)	
Ni(2)-N(4)	2.087(3)		Ni(2)-O(23)	2.089(3)	
Ni(2)-O(9)	2.090(3)		Ni(2)-N(11)	2.100(4)	
Ni(2)-O(10)	2.147(3)		Ni(2)-O(37)	2.110(3)	

Bond Angles [deg]

	(**1**)			(**3**)	
O(1)-Ni(1)-O(5)	177.55(11)		O(20)-Ni(1)-O(34)	178.74(12)	
O(1)-Ni(1)-N(2)	82.12(11)		O(20)-Ni(1)-N(15)	81.88(13)	
O(5)-Ni(1)-N(2)	97.82(11)		O(34)-Ni(1)-N(15)	96.90(13)	
O(1)-Ni(1)-O(12)	87.82(11)		O(20)-Ni(1)-O36	90.74(12)	
O(5)-Ni(1)-O(12)	89.83(10)		O(34)-Ni(1)-O(36)	89.95(11)	
N(2)-Ni(1)-O(12)	105.40(12)		N(15)-Ni(1)-O(36)	107.12(13)	
O(1)-Ni(1)-O(11)	93.83(11)		O(20)-Ni(1)-O(34^i)	97.26(12)	
O(5)-Ni(1)-O(11)	88.61(10)		O(34)-Ni(1)-O(34^i)	83.85(12)	
N(2)-Ni(1)-O(11)	84.55(12)		N(15)-Ni(1)-O(34^i)	168.25(13)	
O(12)-Ni(1)-O(11)	170.05(10)		O(36)-Ni(1)-O(34^i)	84.59(12)	
O(1)-Ni(1)-O(5^i)	96.22(10)		O(20)-Ni(1)-O(18)	92.51(12)	
O(5)-Ni(1)-O(5^i)	84.29(10)		O(18)-Ni(1)-O(34)	87.01(11)	
N(2)-Ni(1)-O(5^i)	169.38(12)		N(15)-Ni(1)-O(18)	83.99(13)	
O(12)-Ni(1)-O(5^i)	84.96(10)		O(18)-Ni(1)-O(36)	168.77(12)	
O(11)-Ni(1)-O(5^i)	85.11(10)		O(18)-Ni(1)-O(34^i)	84.34(11)	

O(1)-Ni(2)-O(2)	89.28(11)	O(20)-Ni(2)-O(26)	90.24(13)
O(1)-Ni(2)-O(4)	90.16(10)	O(20)-Ni(2)-O(35^i)	89.57(12)
O(2)-Ni(2)-O(4)	93.63(10)	O(26)-Ni(2)-O(35^i)	88.93(12)
O(1)-Ni(2)-N(4)	84.61(12)	O(20)-Ni(2)-O(23)	91.93(13)
O(2)-Ni(2)-N(4)	93.53(12)	O(26)-Ni(2)-O(23)	175.87(13)
O(4)-Ni(2)-N(4)	171.08(12)	O(35^i)-Ni(2)-O(23)	94.59(13)
O(1)-Ni(2)-O(9)	172.28(11)	O(20)-Ni(2)-N(11)	84.73(13)
O(2)-Ni(2)-O(9)	90.89(11)	O(26)-Ni(2)-N(11)	94.18(13)
O(4)-Ni(2)-O(9)	82.12(10)	O(35^i)-Ni(2)-N(11)	173.51(13)
N(4)-Ni(2)-O(9)	103.08(12)	O(23)-Ni(2)-N(11)	82.53(14)
O(1)-Ni(2)-O(10)	92.23(11)	O(20)-Ni(2)-O(37)	173.07(13)
O(2)-Ni(2)-O(10)	172.55(11)	O(26)-Ni(2)-O(37)	95.00(13)
O(4)-Ni(2)-O(10)	93.66(11)	O(35^i)-Ni(2)-O(37)	86.01(13)
N(4)-Ni(2)-O(10)	79.35(12)	O(23)-Ni(2)-O(37)	83.13(13)
O(9)-Ni(2)-O(10)	88.60(11)	N(11)-Ni(2)-O(37)	99.37(14)

40

Table of Contents

Hydrolytically active tetranuclear [Ni$^{II}_2$]$_2$ complexes: synthesis, structure, spectroscopy and phosphoester hydrolysis
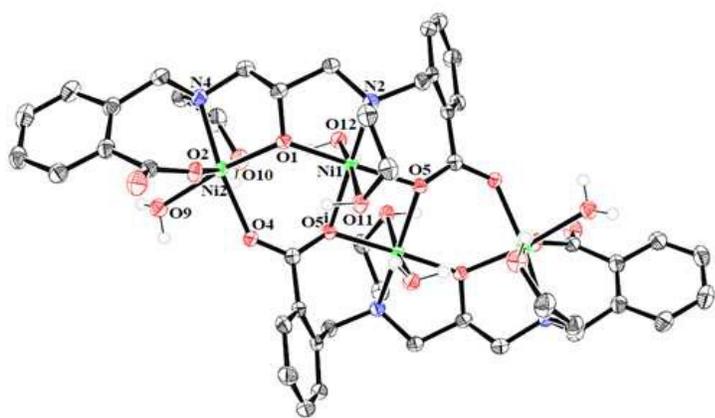
Gopal C. Giri,[a] Ayan Patra,[a] Gonela Vijaykumar,[b] Luca Carrella,[c] and Manindranath Bera[*a]

[a]*Department of Chemistry, University of Kalyani, Kalyani, West Bengal-741235, INDIA. E-mail: mbera2009@klyuniv.ac.in; http://www.klyuniv.ac.in; Fax: +91 33 25828282; Tel: +91 33 25828282 x306*
[b]*Department of Chemical Sciences, Indian Institute of Science Education & Research Kolkata, Mohanpur, West Bengal-741246, INDIA.*
[c]*Institut fur Anorganische Chemie und Analytische Chemie, Johannes-Gutenberg Universität Mainz, Duesbergweg 10-14, D-55128 Mainz, Germany.*

_____

Hydrolytically active three tetranuclear nickel(II) complexes of a new symmetrical μ-bis(tetradentate) ligand, H$_5$chdp were prepared and their catalytic activity toward the phosphoester hydrolysis was examined.

Complex 1